

Article

Generating Continuous Rainfall Time Series with High Temporal Resolution by Using a Stochastic Rainfall Generator with a Copula and Modified Huff Rainfall Curves

Dinh Ty Nguyen¹ and Shien-Tsung Chen^{2,*} 

¹ Ph.D. Program for Civil Engineering, Water Resources Engineering, and Infrastructure Planning, Feng Chia University, Taichung City 407, Taiwan; dinhtybkdn@gmail.com

² Department of Hydraulic and Ocean Engineering, National Cheng Kung University, Tainan City 701, Taiwan

* Correspondence: chen@gs.ncku.edu.tw

Abstract: In this study, a stochastic rainfall generator was developed to create continuous rainfall time series with a high temporal resolution of 10 min. The rainfall-generation process involved Monte Carlo simulation for stochastically generating rainfall parameters such as rainfall quantity, duration, inter-event time, and type. A bivariate copula was used to preserve the correlation between rainfall quantity and rainfall duration in the generated rainfall series. A modified Huff curve method was used to overcome the drawbacks of rainfall type classification by using the conventional Huff curve method. The number of discarded rainfall events was lower in the modified Huff curve method than in the conventional Huff curve method. Moreover, the modified method includes a new rainfall type that better represents rainfall events with a relatively uniform temporal pattern. The developed rainfall generator was used to reproduce rainfall series for the Yilan River Basin in Taiwan. The statistical indices of the generated rainfall series were close to those of the observed rainfall series. The results obtained for rainfall type classification indicated the necessity and suitability of the proposed new rainfall type. Overall, the developed stochastic rainfall generator can suitably reproduce continuous rainfall time series with a resolution of 10 min.

Keywords: stochastic rainfall generator; Huff rainfall curve; copula



Citation: Nguyen, D.T.; Chen, S.-T. Generating Continuous Rainfall Time Series with High Temporal Resolution by Using a Stochastic Rainfall Generator with a Copula and Modified Huff Rainfall Curves. *Water* **2022**, *14*, 2123. <https://doi.org/10.3390/w14132123>

Academic Editors: Fi-John Chang, Li-Chiu Chang and Jui-Fa Chen

Received: 19 May 2022

Accepted: 1 July 2022

Published: 3 July 2022

Publisher's Note: MDPI stays neutral with regard to jurisdictional claims in published maps and institutional affiliations.



Copyright: © 2022 by the authors. Licensee MDPI, Basel, Switzerland. This article is an open access article distributed under the terms and conditions of the Creative Commons Attribution (CC BY) license (<https://creativecommons.org/licenses/by/4.0/>).

1. Introduction

A stochastic rainfall generator is a statistical model that produces synthetic rainfall time series with desired statistical properties. Synthetic rainfall time series can be used for various purposes, such as rainfall–runoff modeling [1,2], design flood estimation [3–5], rainfall projection under climate change scenarios [6–8], and prediction in ungauged basins [9,10]. The Richardson-type rainfall generator [11,12], a popular stochastic rainfall generator, can reproduce long-term continuous daily precipitation time series. This generator uses Markov chains to determine the occurrence of wet or dry days and then simulates the rainfall quantity on wet days through Monte Carlo techniques. Although the aforementioned generator has been proven to be successful in reproducing daily precipitation time series, it cannot be used to obtain sub-daily or high-temporal-resolution rainfall time series.

High-temporal-resolution rainfall data can be used for different purposes, such as analyzing short-duration extreme rainfall events and simulating floods in small catchment areas. To generate rainfall time series with high temporal resolution [13,14], the temporal characteristics of a rainfall event must be determined. High-temporal-resolution rainfall data can be generated using two models: the profile- and pulse-based models. The profile-based model combines the total rainfall quantity and rainfall profile (rainfall type) to obtain a rainfall hyetograph. Typical rainfall types include rainfall described by the Chicago curve [15], Huff curve [16], and triangular curve [17]. The pulse-based model considers a rainfall event to consist of a cluster of rain cells whose occurrences follow a Poisson

distribution. Rodriguez-Iturbe et al. [18,19] examined two popular pulse-based models in detail: the Neyman–Scott cluster model [20–25] and Bartlett–Lewis cluster model [26–31].

In the present study, the profile-based model with Huff rainfall curves, proposed by Huff [16] and modified by Huff and Vogel [32] and Huff [33], was adopted. Huff rainfall curves are presented using four types of dimensionless cumulative hyetographs according to the quarter in which the peak rainfall intensity occurs. Huff curves are popularly used in design storm, runoff simulation, design flood, and rainfall predictions [34–40]. However, Huff curves are not representative of rainfall events with uniform temporal distribution, and the rainfall type cannot be determined when a rainfall event has multiple peak intensities. Therefore, this paper proposes modified Huff rainfall curves for solving the limitations of the original Huff curves. The modified Huff rainfall curves have an additional rainfall type to account for rainfall events with uniform temporal distribution and can be used to classify rainfall events with multiple peak intensities. The proposed rainfall generator uses Monte Carlo simulation for stochastically generating modified Huff rainfall curves and other rainfall parameters (rainfall quantity, duration, and inter-event time) to form continuous rainfall time series with a temporal resolution of 10 min.

A suitable rainfall generator should reproduce rainfall data with anticipated statistical properties. Usually, a single rainfall parameter can be suitably generated through Monte Carlo simulation with an appropriate marginal distribution. However, various rainfall parameters can be interrelated. For example, a rainfall event with a longer duration is typically associated with higher cumulative rainfall. Therefore, the generation of rainfall parameters individually may result in the correlation between rainfall variables being lost and distorted rainfall data being obtained. Hence, the present study used a copula [41] to account for the correlation between parameters during the rainfall generation process. Copulas are mathematical functions that model the dependence among interrelated variables. An advantage of a copula is that it allows the dependence structure of variables to be modeled without the selection of marginal distributions. Therefore, copulas are widely employed in frequency analysis in hydrology [42–48]. The present study examined the correlation between rainfall parameters and constructed copulas for rainfall quantity and duration to generate rainfall data with appropriate correlation properties.

The remainder of this paper is structured as follows. The basic structure of the proposed continuous rainfall generator, the copula theory, and the modified Huff rainfall curves are described in Section 2. Section 3 presents information on the study area, the Yilan River Basin in Taiwan, and the collected 10 min rainfall data. Section 4 details the development of the proposed stochastic rainfall generator, with a focus on the modified Huff rainfall curves and adopted copula functions. The rainfall-generation results are presented in Section 5, and the conclusions of this study are provided in Section 6.

2. Methodology

2.1. Continuous Rainfall Time Series Generation

In this study, a stochastic rainfall generator was developed to produce a continuous rainfall time series with a high temporal resolution of 10 min. A continuous rainfall time series contains data for alternate wet and dry periods. The wet period indicates a rainfall event, and the dry period is called the inter-event time. A rainfall event can be characterized by rainfall duration, quantity, and type. Therefore, a continuous rainfall time series contains data related to four parameters: total rainfall quantity (R), rainfall duration (D), rainfall type, and rainfall inter-event time (T) (Figure 1).

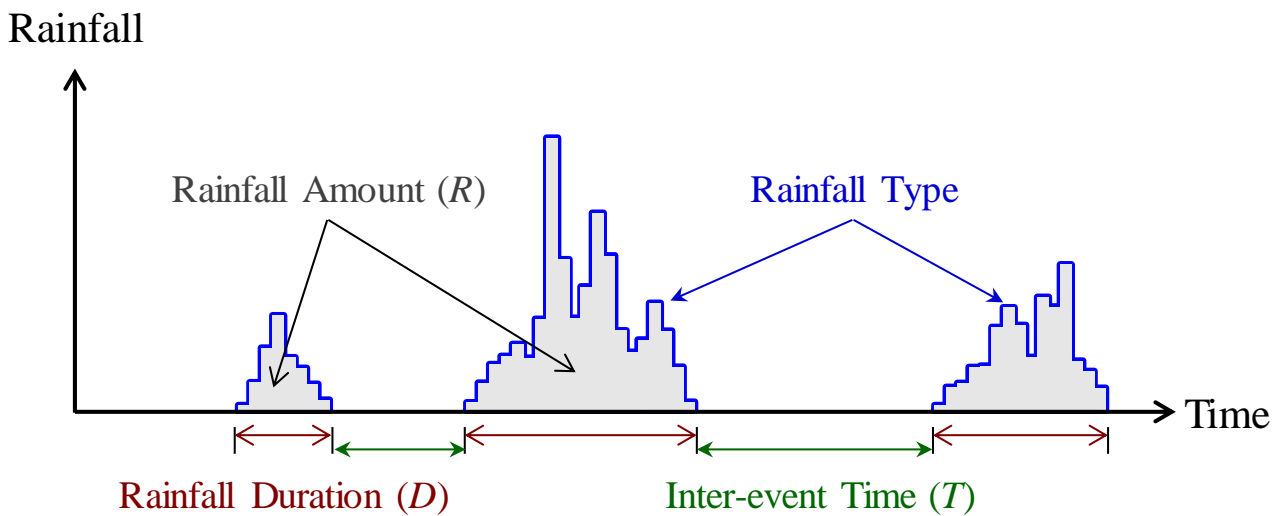


Figure 1. Example of rainfall time series and parameters.

In this study, the generation of continuous rainfall time series basically involved Monte Carlo simulation. First, the statistical properties and probability distribution of the four rainfall parameters were obtained and analyzed. Subsequently, on the time coordinate, an alternating sequence of rainfall duration and rainfall inter-event time was randomly generated according to their statistical properties and probability distributions. Total rainfall quantity, rainfall type and rainfall duration were generated simultaneously to construct a rainfall event. Because of the statistical correlation between rainfall quantity and duration, the copula method (Section 2.2) was used for simultaneously producing rainfall quantity and duration data. Moreover, modified Huff rainfall curves (Section 2.3) were used for better describing the temporal distribution of rainfall data. By using a repetitive generation process based on Monte Carlo simulation, continuous rainfall time series with the desired length were constructed.

2.2. Bivariate Copula

A copula is a multivariate distribution function that links the univariate distribution functions of each random variable. Copulas, originally introduced in the theorem proposed by Sklar [41], can model the correlation among variables without the assumptions made about the marginal distributions. According to this theorem, the joint cumulative distribution function F_{XY} of random variables X and Y with respect to the marginal cumulative distribution functions F_X and F_Y can be expressed as follows:

$$F_{XY}(x, y) = C(F_X(x), F_Y(y)) = C(u, v) \tag{1}$$

where C is a bivariate copula, and u and v are the cumulative probabilities of x and y , respectively. Let $\mathbf{I} = [0, 1]$, and let the bivariate copula C be a mapping function defined on a unit square, where $C : [0, 1]^2 \rightarrow \mathbf{I}$. When F_X and F_Y are continuous, a unique copula representation exists. Thus, F_{XY} defines a joint distribution function with the marginal distributions F_X and F_Y [49]. For any u and v in $\mathbf{I} = [0, 1]$, the copula is bounded as follows:

$$C(u, 0) = 0, C(0, v) = 0, C(u, 1) = u, C(1, v) = v \tag{2}$$

The aforementioned copula satisfies the two-increasing property; thus, for all $u_1 \leq u_2$ and $v_1 \leq v_2$, the following equation is satisfied:

$$C(u_2, v_2) - C(u_2, v_1) - C(u_1, v_2) + C(u_1, v_1) \geq 0 \tag{3}$$

Copulas are categorized into various families. The Archimedean copula family is popular in hydrology because of its simplicity and practicality in application [3,50–52]. This family includes various copulas with different numbers of parameters. Salvadori and De Michele [53,54] and Genest and Favre [55] suggested the use of one-parameter copulas in hydrology. The present study adopted three commonly used one-parameter (θ) copulas from the Archimedean copula family: the Frank, Clayton, and Gumbel copulas. The parameter θ can be calculated from the relationship between θ and Kendall’s tau (τ), which is the rank correlation coefficient. Table 1 lists the copula functions adopted in this study and the relationships between θ and τ for these functions [56].

Table 1. Three copula functions used in this study and the relationships between θ and τ for these functions.

Copula	Function	Parameter Space	Relationship between θ and τ
Clayton	$C(u, v) = (u^{-\theta} + v^{-\theta} - 1)^{-1/\theta}$	$\theta > 0$	$\tau = \frac{\theta}{\theta+2}$
Frank	$C(u, v) = -\frac{1}{\theta} \ln \left\{ 1 + \frac{[\exp(-\theta u) - 1] \cdot [\exp(-\theta v) - 1]}{\exp(-\theta) - 1} \right\}$	$\theta \neq 0$	$\tau = 1 + \frac{4}{\theta} \left[\frac{1}{\theta} \int_0^\theta \frac{t}{\exp(t) - 1} dt - 1 \right]$
Gumbel	$C(u, v) = \exp \left\{ - \left[(-\ln u)^\theta + (-\ln v)^\theta \right]^{1/\theta} \right\}$	$\theta \geq 1$	$\tau = 1 - \frac{1}{\theta}$

2.3. Modified Huff Rainfall Curves

Profile-based models typically use Huff rainfall curves as the basis for defining the temporal distribution of rainfall events. These curves are empirical and dimensionless, probabilistic representations of cumulative hyetographs. The temporal rainfall patterns were classified into four types (Type 1 to Type 4) according to the time when the peak intensity occurred (i.e., in the first, second, third, or fourth quarter of rainfall duration). Figure 2 presents the temporal patterns, median (solid line), and 10% and 90% cumulative probabilities (lower and upper dashed lines, respectively) of the four types of Huff curves. The cumulative rainfall depth and cumulative rainfall duration were standardized by the total rainfall depth and total rainfall duration, respectively, and are presented in dimensionless form within the interval from 0% to 100%.

Although Huff rainfall curves are popular because of their ease of use, they have certain limitations. First, if a rainfall event has multiple peak intensities, then the rainfall type cannot be determined, and this event is omitted or randomly classified into one of the four rainfall types [57]. Second, a rainfall event with a relatively uniform temporal distribution cannot be well-represented by the four Huff curves. This paper proposes the solution described in the following text to the problem caused by the existence of multiple peak rainfall intensities. When a rainfall event has multiple peak intensities, the maximum total rainfall in a quarter instead of the peak intensity should be used to determine the rainfall type. However, a rainfall event with multiple peak intensities and the same maximum total rainfall in two or more quarters cannot be classified using the aforementioned solution. Nevertheless, this type of rare event occupies a very small portion of rainfall time series. Because Huff curves cannot be used to designate a rainfall event with a relatively uniform temporal distribution, this paper proposes an additional rainfall type (Type 5) for labeling such a rainfall event. The Schutz index (explained in the following paragraph) was used to distinguish Type 5 rainfall events from the other types of rainfall events.

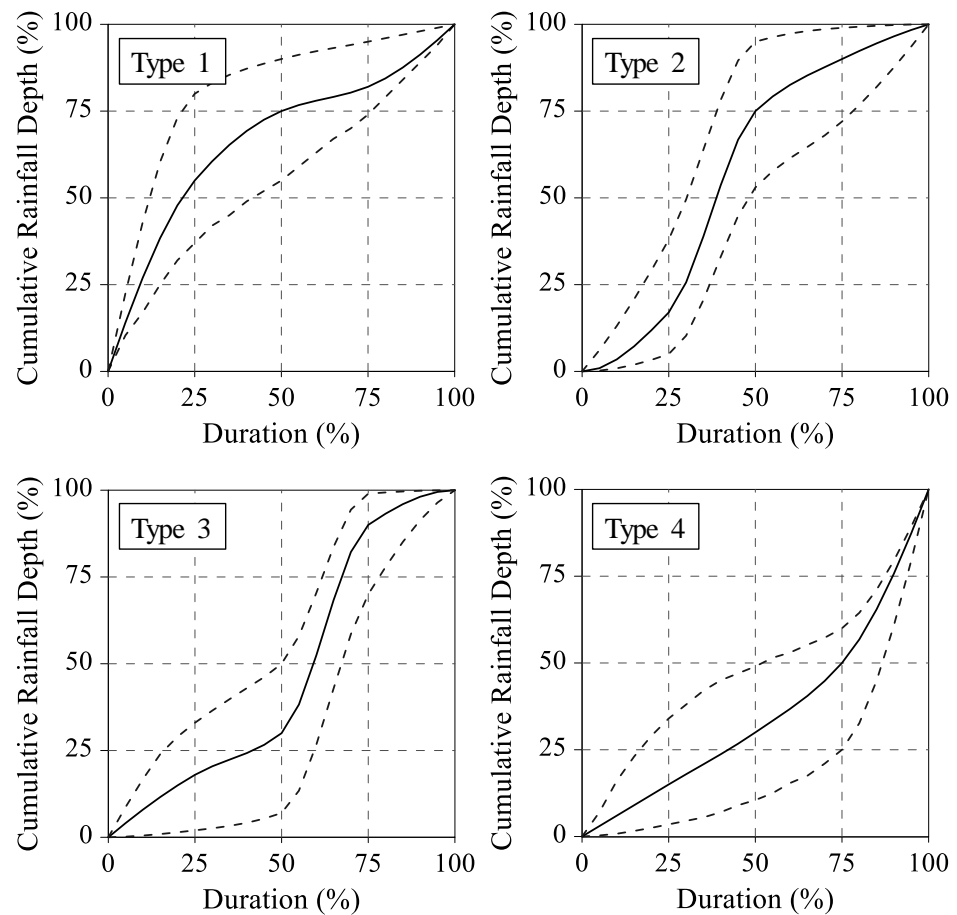


Figure 2. Huff’s four rainfall types with the corresponding median (solid line) and 10% and 90% cumulative probabilities (lower and upper dashed lines, respectively).

The Schutz index [58] was originally proposed as an equity measure for income metrics in economics. Therefore, the Schutz index is an appropriate measure for assessing the uniformity of a distribution. Schutz [58] proposed the aforementioned index on the basis of the Lorenz curve [59], which is a probability plot with respect to a variable accumulated in a nondecreasing order. Figure 3 illustrates a Lorenz curve for income distribution among a population. Figure 3a depicts the histogram of the income of each 10% of the population versus the cumulative population in a nondecreasing order (the unit of income and population is percentage in this graph). By accumulating the income with respect to the population, the Lorenz curve (the red curve in Figure 3b) can be obtained. The 45° diagonal in Figure 3b indicates the perfect-equity income. When the Lorenz curve is close to the 45° diagonal, a uniform income distribution is identified. The Schutz index is an objective measure of the closeness of the Lorenz curve to the line of perfect equity. Thus, the Schutz index quantifies the total deviation of the income of each category (y_i) from the mean income (y_{mean}). Figure 4 presents an example of a rainfall event to describe the calculation of the Schutz index. The rainfall in each time step (y_i) of an original event is sorted and rearranged in a nondecreasing order, where $i = 1, 2, \dots, n$, and n is the last time step. The Schutz index (S) is calculated using the following equation:

$$S = \frac{1}{2} \cdot \frac{\sum_{i=1}^n |y_i - y_{mean}|}{\sum_{i=1}^n y_i} \tag{4}$$

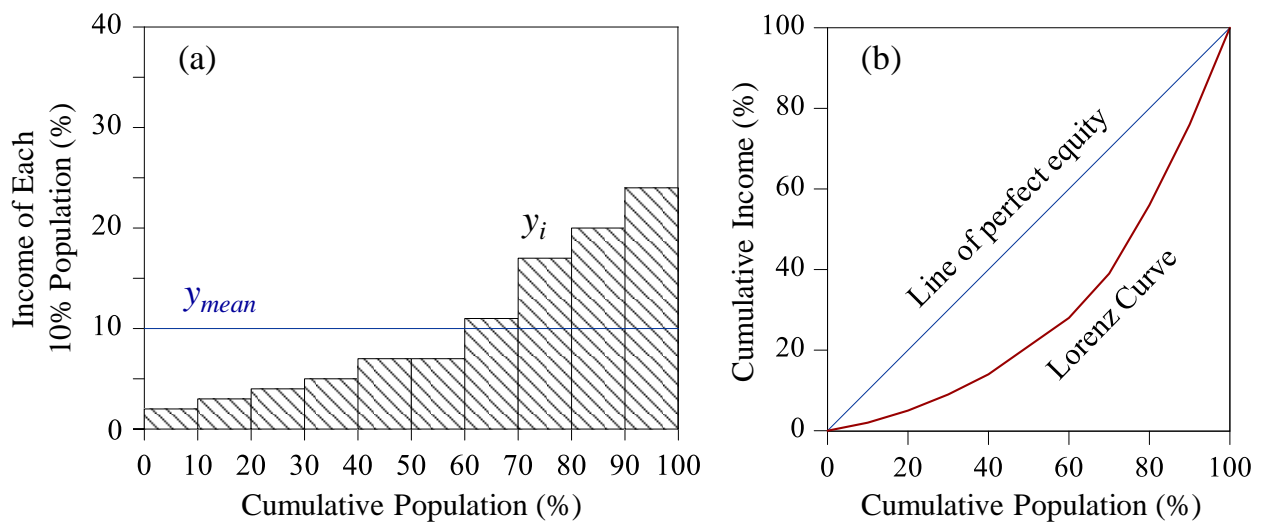


Figure 3. Example of the derivation of a Lorenz curve: (a) income of each 10% of the population arranged in a nondecreasing order and (b) comparison of the Lorenz curve and the line of perfect equity.

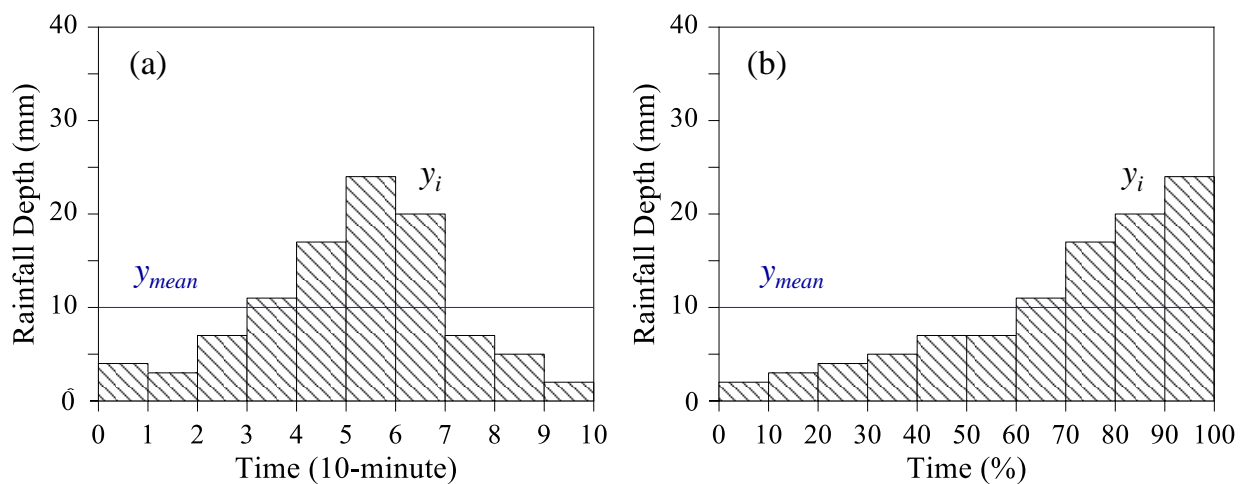


Figure 4. Example of the calculation of the Schutz index by using rainfall data: (a) original rainfall event and (b) sorted nondecreasing rainfall depth.

When S is 0, the rainfall in each step (y_i) is the same as the mean rainfall (y_{mean}), and the rainfall distribution is perfectly uniform. Thus, in the aforementioned scenario, the cumulative rainfall pattern corresponds to the diagonal in Figure 3b. When S approaches 1, the rainfall distribution is far from uniform. Thus, a small S value indicates that the rainfall distribution can be categorized as Type 5 (uniform rainfall distribution), and a large S value suggests that the rainfall distribution belongs to one category among Types 1 to 4. The modified Huff curve method is illustrated in Figure 5. First, the Schutz index (S) of a rainfall event is calculated to determine whether the rainfall distribution is uniform. If S is smaller than a threshold (which is determined in the following section), the rainfall distribution is considered to be uniform and categorized as Type 5. If S is larger than the threshold, the rainfall distribution is not close to Type 5 and belongs to one category among Types 1 to 4. In this circumstance, the existence of multiple peak rainfall intensities is checked. If only one peak intensity exists, the conventional Huff method is used to identify the rainfall type. If multiple peak intensities exist, the maximum total rainfall in a quarter is used to determine the rainfall type.

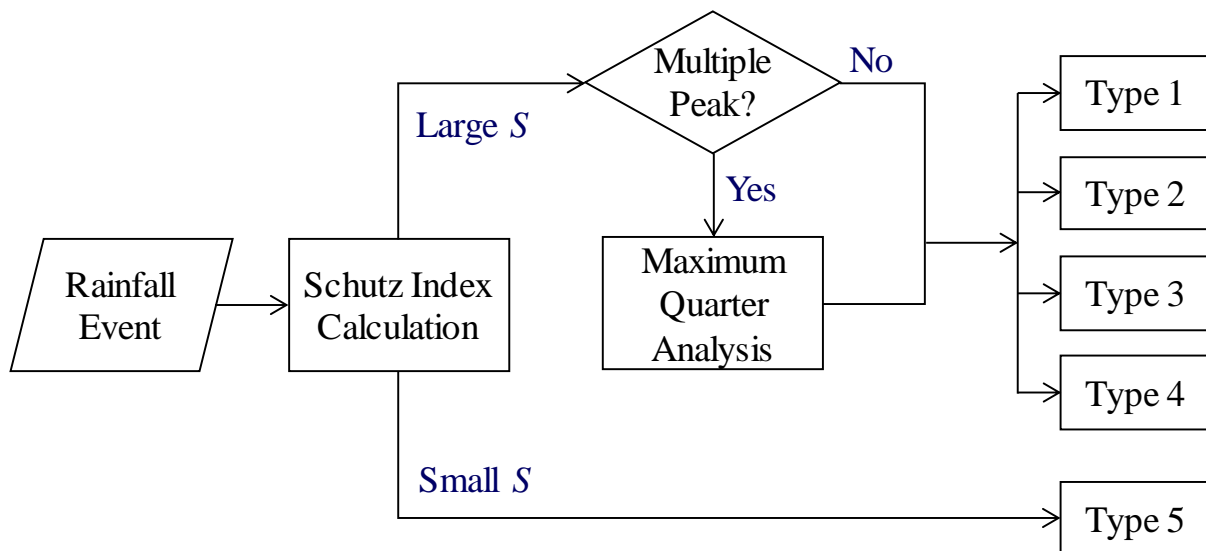


Figure 5. Process of the modified Huff method for determining the rainfall type.

3. Study Area and Rainfall Data

In this study, 10 min rainfall data from 2012 to 2018 were collected for the Yilan River Basin in Taiwan. The Yilan River’s watershed is located in northeastern Taiwan (Figure 6), where the typical climate is humid and rainy. Nine rain gauges collect 10 min rainfall data for the Yilan River Basin. As displayed in Figure 6, seven of these rain gauges are located inside the basin, whereas two are located outside the basin.

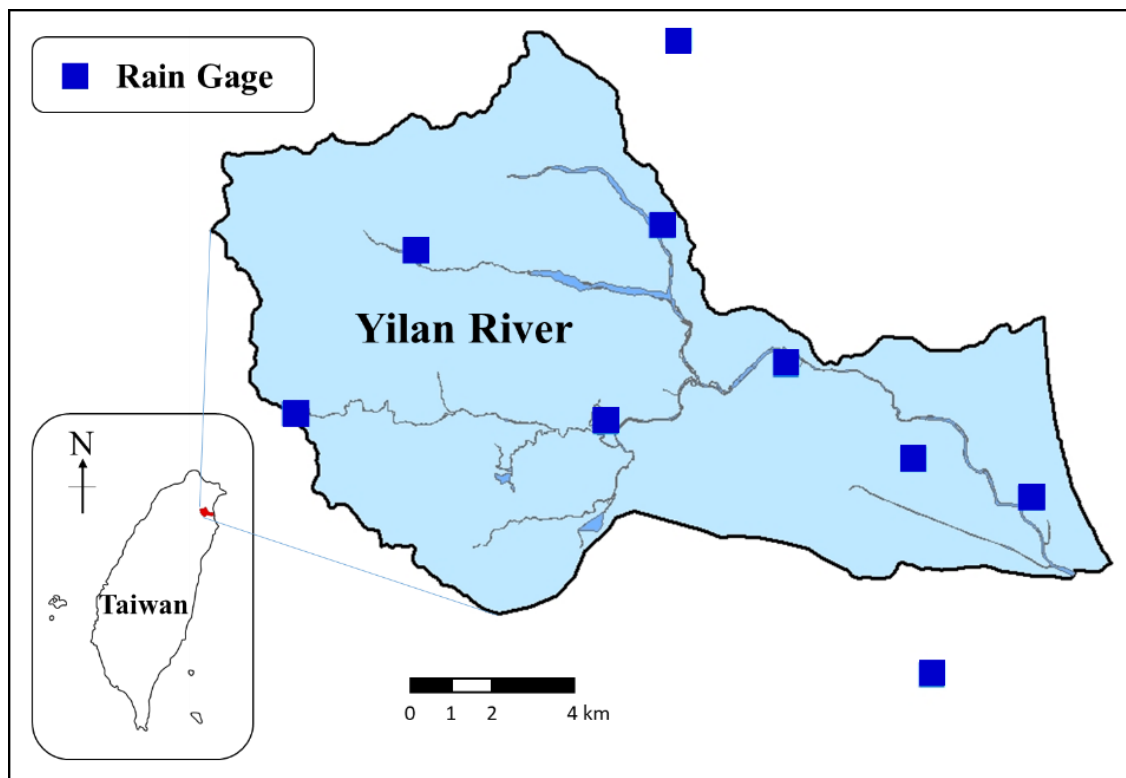


Figure 6. Locations of the study area and rain gauges.

Rainfall time series must be analyzed to obtain their statistical properties. The primary task is to define and distinguish a rainfall event. Researchers have used various methods to

distinguish rainfall events and determine the rainfall inter-event time [60,61]. The selection of minimum rainfall duration and minimum rainfall inter-event time is dependent on the temporal resolution of the available data. Because the time resolution of the data collected in this study was 10 min, and the rainfall types were distinguished according to Huff rainfall curves, the minimum duration of a rainfall event was set as 40 min. Thus, rainfall events shorter than 40 min were not included in the rainfall event database. Moreover, the minimum inter-event time was set as 1 h. Thus, when a dry period was shorter than 1 h, this period and the wet periods preceding and following it were regarded as a rainfall event [62,63]. This approach considerably reduced the number of discarded rainfall events with durations less than 40 min.

Summer and winter monsoons occurred in the study area. Therefore, the rainfall events in this study were divided into those occurring in the summer (from May to October) and winter (from November to April of next year) seasons. A total of 4317 summer rainfall events and 3246 winter rainfall events were identified in this study.

4. Stochastic Rainfall-Generation Model Development

4.1. Rainfall Type

A threshold value of the Schutz index (S) was determined to identify Type 5 rainfall events. No a priori criterion can be used to set the threshold value; however, Bonta and Shahalam [64] suggested using the data of more than 120 storms to obtain stable Huff curves. The present study assumed that the number of Type 5 rainfall events was not greater than the numbers of Type 1 to Type 4 rainfall events. This assumption is rational because the number of rainfall events with a uniform distribution (Type 5) is usually less than those with a nonuniform distribution (Types 1 to 4). Therefore, a grid search method was used for S under the condition of increasing the number of Type 5 rainfall events; however, the number of Type 5 rainfall events was constrained by the minimum number of Type 1 to Type 4 rainfall events. Consequently, the number of Type 5 rainfall events could not exceed the minimum number of Type 1 to Type 4 rainfall events. Table 2 lists the threshold values of S for the summer and winter seasons as well as the numbers and percentages of Type 1 to Type 5 rainfall events. The threshold values for the summer and winter seasons were 0.29 and 0.30, respectively. By using the derived thresholds and the process described in the previous section (Figure 5), the identified rainfall events were categorized into different types. Figure 7 shows the classification of rainfall types for the summer season by using modified Huff rainfall curves. The bold black curves connecting squares, circles, and triangles indicate the 10%, 50%, and 90% percentiles of the rainfall categories, respectively. The colored curves represent the observed rainfall distributions. The rainfall classification curves obtained for the winter season were analogous to those obtained for the summer season. In Figure 7, the Type 5 rainfall events exhibit the characteristic of uniform distribution, which is different from the characteristics of Type 1 to Type 4 rainfall events. The results displayed in Figure 7 support the rationale that the Type 5 category is essential for better representing a uniform rainfall distribution.

Table 2. Threshold values of the Schutz index as well as the numbers and percentages of Type 1 to Type 5 rainfall events.

	Summer Season		Winter Season	
	Number of Events	Percentage (%)	Number of Events	Percentage (%)
Type 1	1069	24.76	869	26.77
Type 2	1003	23.24	721	22.21
Type 3	857	19.85	610	18.79
Type 4	704	16.31	534	16.45
Type 5	684	15.84	512	15.78
Schutz index		0.29		0.30

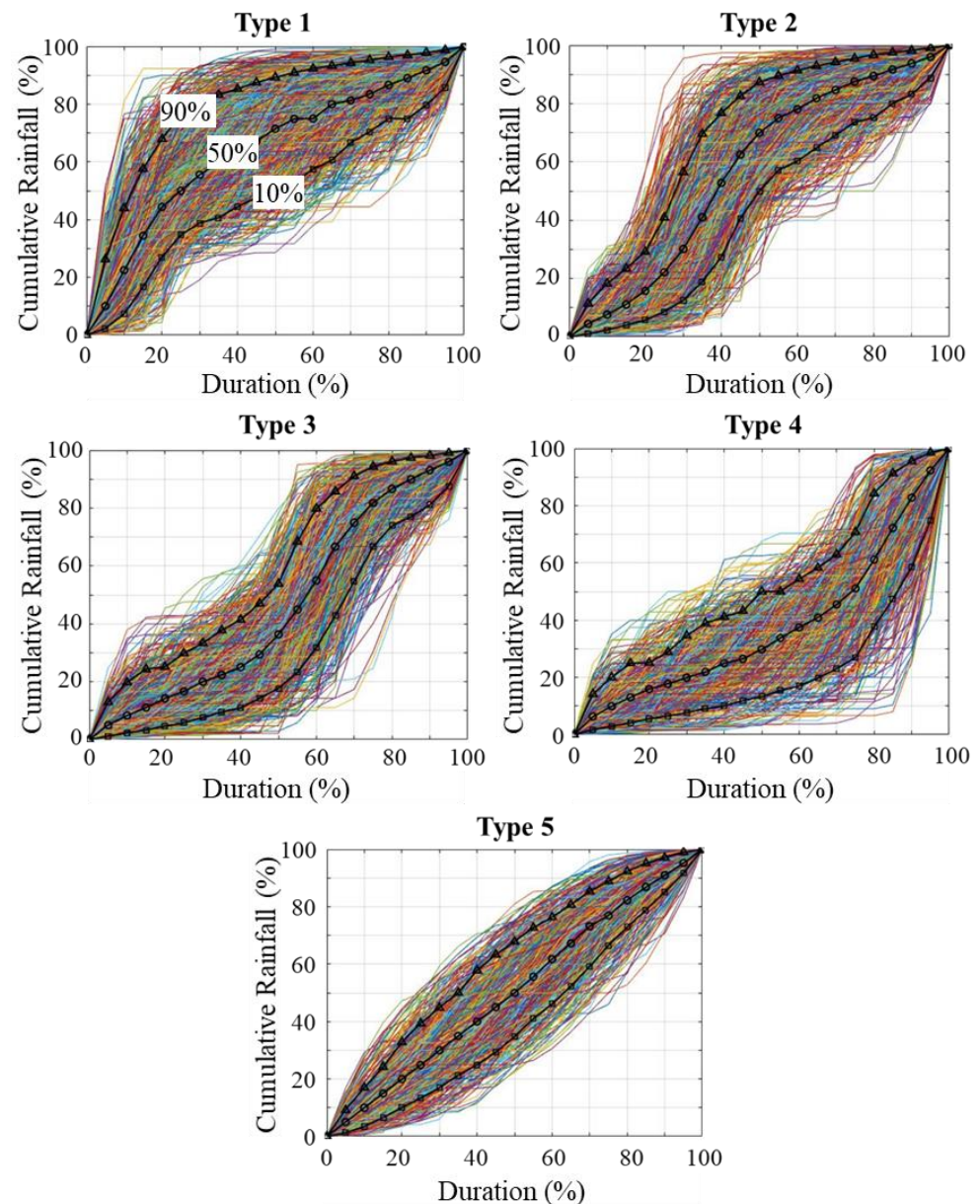


Figure 7. Summer rainfall events categorized using the modified Huff method.

In the traditional Huff method, approximately 40% of the identified rainfall events would need to be ignored because they are associated with multiple peak rainfall intensities. However, in the proposed method, only 5% of the identified rainfall events were ignored.

4.2. Copula Function

This study examined the correlation between each pair of the rainfall parameters by using normalized rank scatter plots [48]. The rainfall quantity, duration, and inter-event time were normalized between 0 and 1 and sorted in ascending order. These normalized and sorted data were then used to draw scatter plots. Figure 8 displays the normalized rank scatter plots for different pairs of rainfall parameters in the summer season. The rows in this figure indicate different rainfall types (Types 1 to 5), and the three columns denote three pairs of parameters. The patterns in the first column in Figure 8 indicate that the rainfall quantity and duration (R, D) are correlated, especially for large values. However, the patterns in the second and third columns suggest that no correlation exists between rainfall duration and inter-event time (D, T) and between rainfall quantity and inter-event

time (R, T), respectively. The normalized rank scatter plots for the winter season are similar to those for the summer season and thus are not shown in this paper. Pearson correlation coefficients were calculated using the data in the rank-normalized plots to quantify the correlation between the rainfall parameters. The average correlation coefficients for (R, D) in the summer and winter seasons were 0.70 and 0.85, respectively. However, the correlation coefficients for (D, T) and (R, T) were close to 0. Therefore, the rainfall quantity and duration (R, D) were adopted to construct a bivariate copula for rainfall generation.

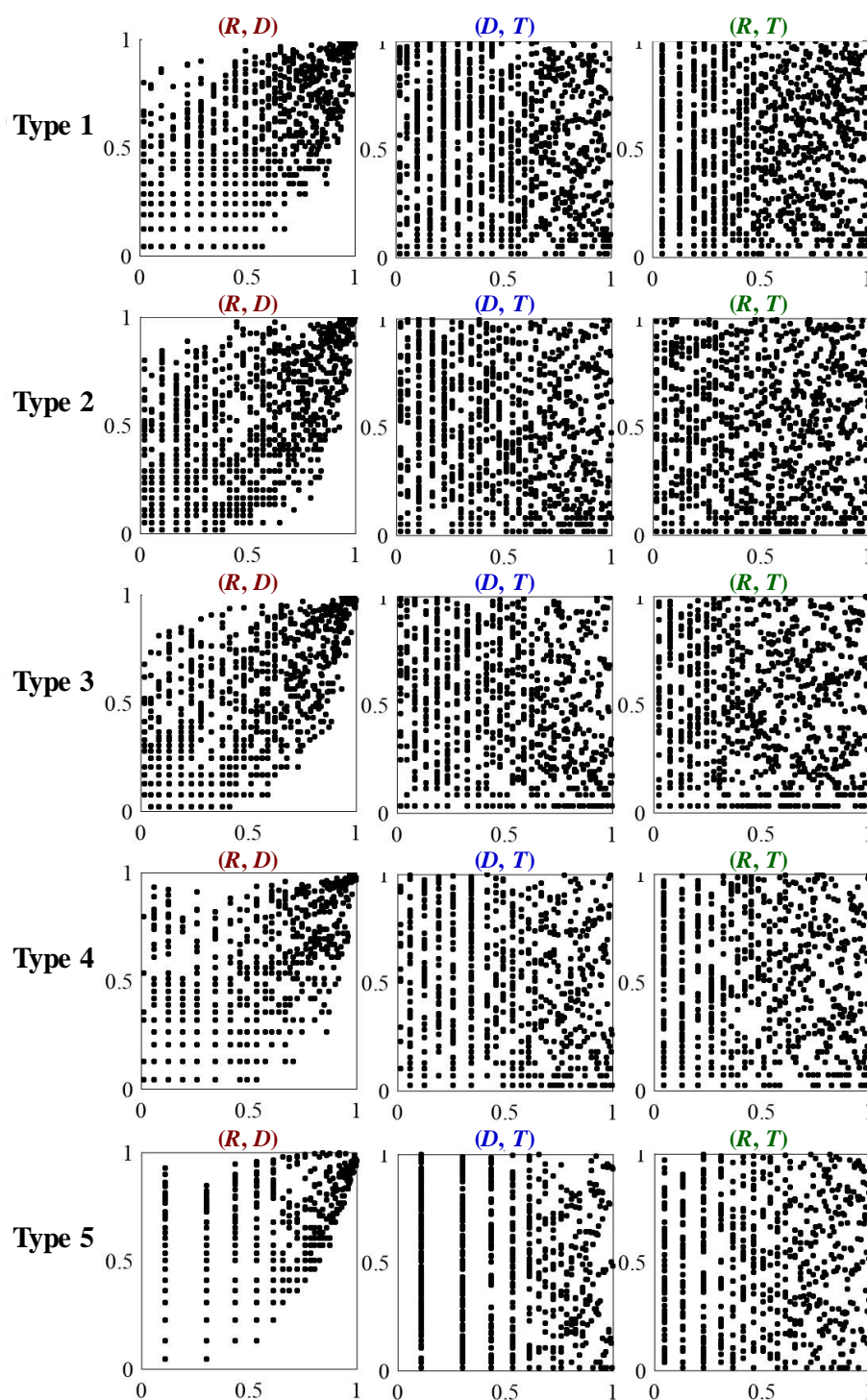


Figure 8. Normalized-rank scatter plots for different pairs of rainfall parameters in summer.

The next step involved determining which bivariate distribution function (from among the Frank, Clayton, and Gumbel copulas) was best suited for describing the correlation between the rainfall quantity and duration in the study area. Kendall’s tau (τ) was calculated and used to determine the θ value of the three copulas adopted in this study (Table 1). The τ and θ values derived for the three copulas are listed in Table 3. After deriving the aforementioned values, the three copulas were used to model the correlation between rainfall quantity and rainfall duration. The cumulative probability functions of the three copulas for the summer season are illustrated in Figure 9. The blue, red, and green curves indicate the cumulative probability functions of the Clayton, Frank, and Gumbel copulas, respectively. The black dotted line represents the cumulative probability function of the empirical copula, which was constructed using the observed rainfall quantity and duration. The Clayton, Frank, Gumbel, and empirical copulas exhibited similar patterns to each other except for the Type 5 rainfall data under low cumulative probabilities. In general, the Clayton, Frank, and Gumbel copulas can suitably model the correlation between rainfall quantity and rainfall duration. The present study used the root mean square error (RMSE) for objectively determining the copula with the best fit to the empirical copula. Table 4 lists the RMSEs in probability (the vertical axis in Figure 9) for different copulas and rainfall types. The minimum RMSEs are highlighted in bold although some values are the same after being rounded off. The results indicate that the Frank copula was the most appropriate copula for modeling the correlation between the rainfall quantity and duration in the study area.

Table 3. Values of τ and θ for the three copulas in summer and winter.

	Summer Season				Winter Season			
	Kendall’s Tau τ	Parameter θ			Kendall’s Tau τ	Parameter θ		
		Clayton	Frank	Gumbel		Clayton	Frank	Gumbel
Type 1	0.487	1.901	5.510	1.950	0.602	3.021	7.975	2.511
Type 2	0.417	1.428	4.394	1.714	0.633	3.455	8.893	2.727
Type 3	0.465	1.739	5.136	1.870	0.613	3.161	8.273	2.581
Type 4	0.436	1.546	4.680	1.773	0.623	3.307	8.581	2.653
Type 5	0.490	1.920	5.553	1.960	0.743	5.785	13.70	3.892

Table 4. RMSEs in probability values for different copulas and rainfall types.

	Summer Season			Winter Season		
	Clayton	Frank	Gumbel	Clayton	Frank	Gumbel
Type 1	0.030	0.027	0.028	0.038	0.036	0.037
Type 2	0.024	0.019	0.018	0.026	0.024	0.025
Type 3	0.026	0.020	0.020	0.023	0.022	0.022
Type 4	0.034	0.030	0.031	0.042	0.040	0.041
Type 5	0.059	0.059	0.060	0.052	0.052	0.052

Because the rainfall quantity and duration were fitted using the Frank copula, the rainfall inter-event time was modeled using a univariate probability distribution. In this study, the observation data was directly applied to construct the empirical distribution for the rainfall inter-event time.

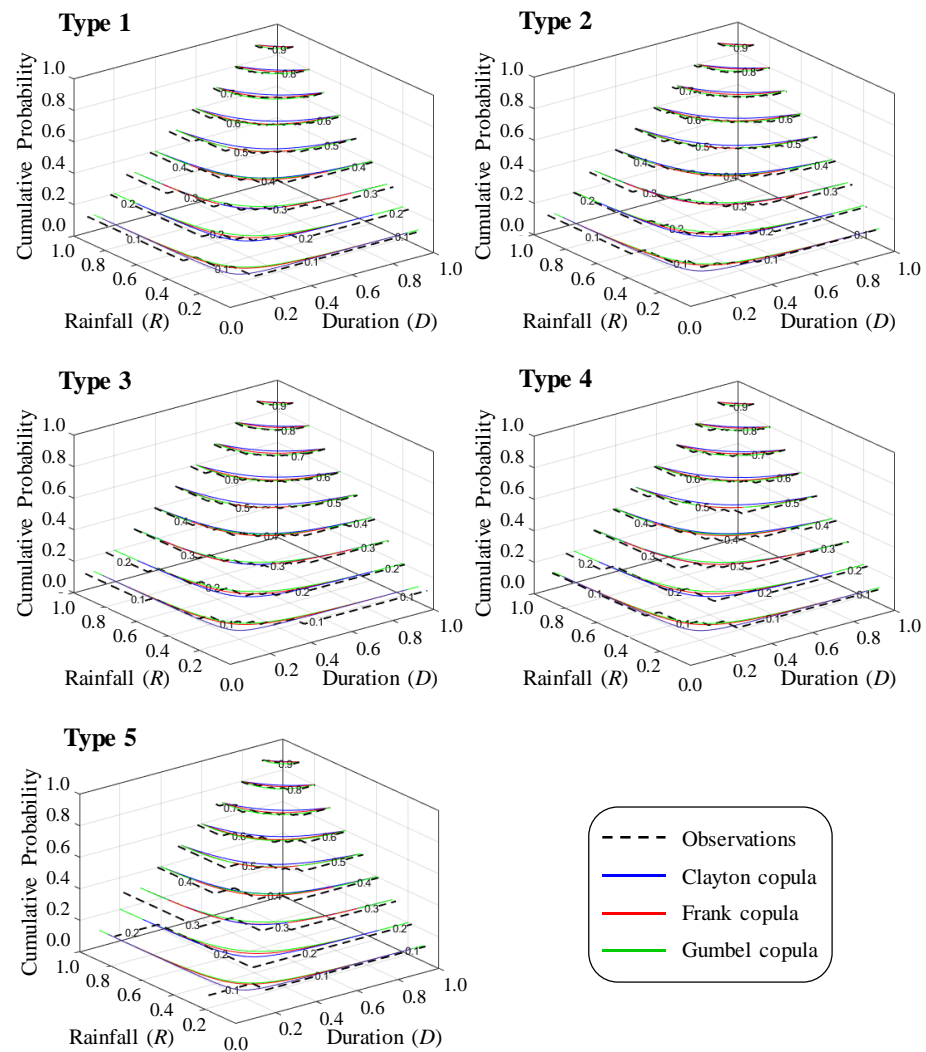


Figure 9. Copula functions for different rainfall types in summer.

4.3. Procedure for Stochastic Rainfall Generation

In this study, rainfall data generation was conducted through Monte Carlo simulation, which involves repeated random sampling. First, a 50% probability is used to determine whether a rainfall time series begins with a rainfall event or rainfall inter-event time. Rainfall events and inter-event times are then alternately produced. To produce a rainfall inter-event time, a number in the range of (0, 1) is randomly generated and substituted into the empirical probability distribution. To produce a rainfall event, three rainfall parameters, namely rainfall quantity, duration, and type, are generated.

The rainfall quantity and duration are generated simultaneously by using the Frank copula. First, a random number is generated as the cumulative probability of the copula, which is represented by a contour curve in Figure 9. Next, a point on the contour curve is randomly selected with equal probability. The values of rainfall quantity and duration can then be obtained from the location of the selected point. For the generation of rainfall type, one out of the five rainfall types (Types 1 to 5) is randomly selected according to their probabilities of occurrence (Table 2). After the rainfall type is determined, a random number is generated as the percentile for that rainfall type (Figure 7). Thus, a rainfall curve can be retrieved for the identified rainfall type with the generated percentile value.

By using the aforementioned process to produce rainfall parameters repetitively, synthetic continuous rainfall time series of any desired length can be generated. This study repeated the aforementioned procedure 10,000 times to generate a continuous rainfall time

series with 10,000 sets of rainfall events and inter-event times. The results of this study are discussed in the following section.

5. Results and Discussion

This paper proposes a methodology for generating a continuous rainfall time series with a temporal resolution of 10 min. The statistical properties of the generated rainfall time series should correspond to those of the observed rainfall time series. The observed rainfall time series from 2012 to 2018 in the study area was used as the database to generate a synthetic rainfall time series. The study area has two main seasons: summer (from May to October) and winter (from November to April of next year). The summer season includes the “plum rain” season (May and June) and typhoon rain season (July to October). The typical rainfall types occurring in the summer season are stationary frontal rainfall, convective rainfall, and typhoon rainfall. The winter season is dominated by the northeast monsoon, which constantly brings moist ocean air into the study area. Short-duration, heavy rainfall is typically received in summer, whereas long-duration, moderate rainfall is typically received in winter.

The statistics of four rainfall parameters were calculated to assess the performance of the proposed rainfall generator. Figure 10 presents the average rainfall quantity and the standard deviation of the rainfall quantity in the summer (red circle) and winter (blue square) seasons. The average and standard deviation were calculated with respect to rainfall type (Types 1 to 5); therefore, five points were obtained for each of the aforementioned parameters in each season. These points lie close to the 45° diagonal, which indicates that the average generated rainfall quantity and the standard deviation of the generated rainfall quantity are analogous to the corresponding observation data. As displayed in Figure 10, the average rainfall quantity and the standard deviation of the rainfall quantity were larger in the summer than in the winter season for all types of rainfall except for Type 5 rainfall (the smallest value represented by a red circle). Type 5 rainfall has a relatively uniform temporal distribution, and Type 5 rainfall events are usually short-duration events with low rainfall quantities. Therefore, in this study, the average rainfall quantity and standard deviation of the rainfall quantity were low for Type 5 rainfall. In general, the aforementioned parameters were larger for Type 2 and Type 3 rainfall than for the other types of rainfall.

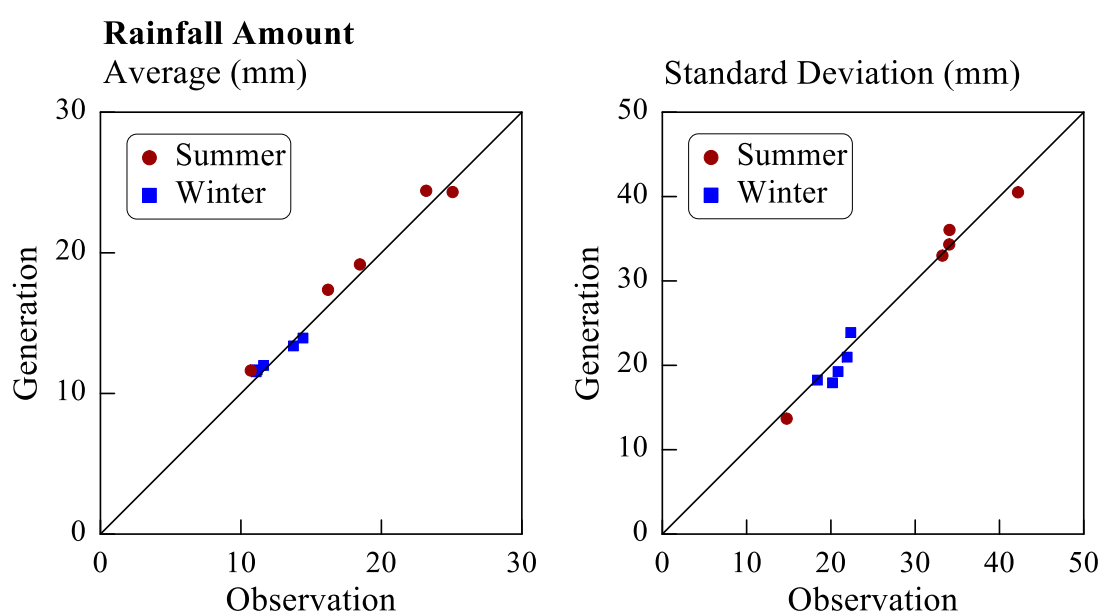


Figure 10. Comparison of the average and standard deviation values obtained for the observed and generated rainfall quantities.

Figure 11 displays the average rainfall duration and the standard deviation of the rainfall duration, and the duration unit in this graph is 10 min. This figure reveals that the average rainfall durations were generally longer in the winter than in the summer season. The shortest average rainfall durations in the summer and winter seasons (the lowest red circle and blue square in the left part of Figure 11) were observed for Type 5 rainfall. Moreover, the standard deviations in winter were larger than those in summer. The aforementioned results correspond to the rainfall characteristics in the study area. The points plotted for the average rainfall duration and the standard deviation of the rainfall duration are close to the 45° diagonal, which indicates that the generated values are close to the observed values. The rainfall quantity and duration were generated using the copula method. Figure 12 illustrates the correlation between the rainfall quantity and the rainfall duration in terms of τ . Positive correlation coefficients were obtained between the aforementioned factors, which indicates that in general, the longer the rainfall duration, the higher the rainfall quantity. The higher correlation in winter than in summer suggests that more persistent rainfall was received for a longer duration in the winter rainfall events than in the summer rainfall events. The lower correlation in summer can be attributed to the various rainfall patterns observed during this season (i.e., frontal, convective, and typhoon rainfalls). Overall, the results displayed in Figures 10–12 indicate that the selected copula can accurately reproduce the correlation between rainfall quantity and rainfall duration.

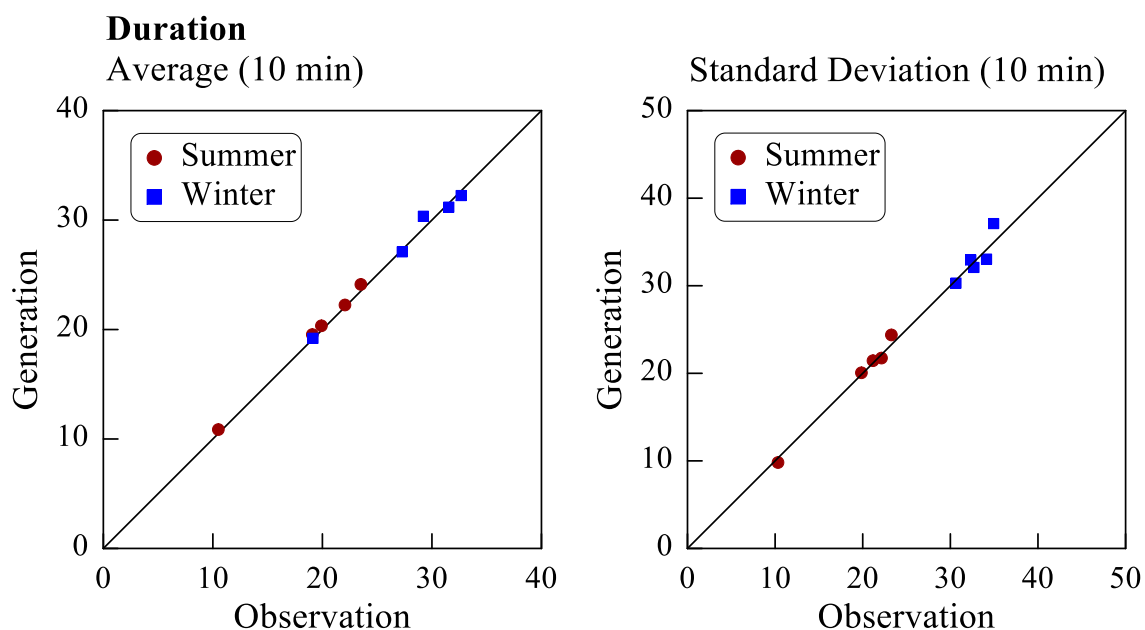


Figure 11. Comparison of the average and standard deviation values obtained for the observed and generated rainfall duration.

Figure 13 presents the average and standard deviation values obtained for the rainfall inter-event time (the time unit in this figure is 10 min). The rainfall inter-event times in the summer and winter seasons were similar (i.e., approximately 3000 min (approximately 2 days)). The developed rainfall generator reproduced the inter-event time on the basis of the empirical probability distribution. The averages of the generated rainfall inter-event times were in line with the corresponding observations; however, the standard deviations were somewhat smaller than the corresponding observations, especially for the winter season. Figure 14 presents the number of rainfall events (in percentage) generated for the different rainfall types. The percentages of rainfall events generated for each rainfall type were close to the corresponding observation data presented in Table 2. In conclusion, the proposed rainfall generation model can suitably reproduce rainfall time series with high temporal resolution.

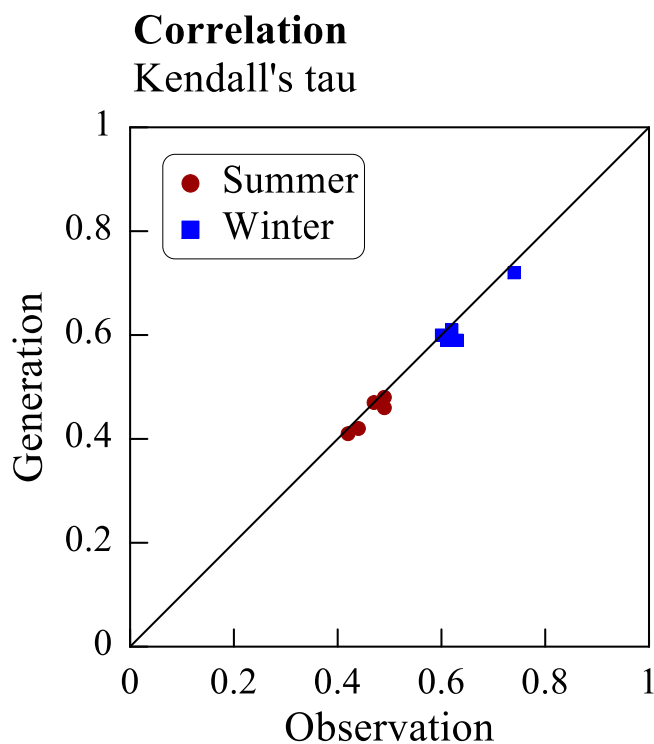


Figure 12. Comparison of the observed and generated correlations between rainfall quantity and duration.

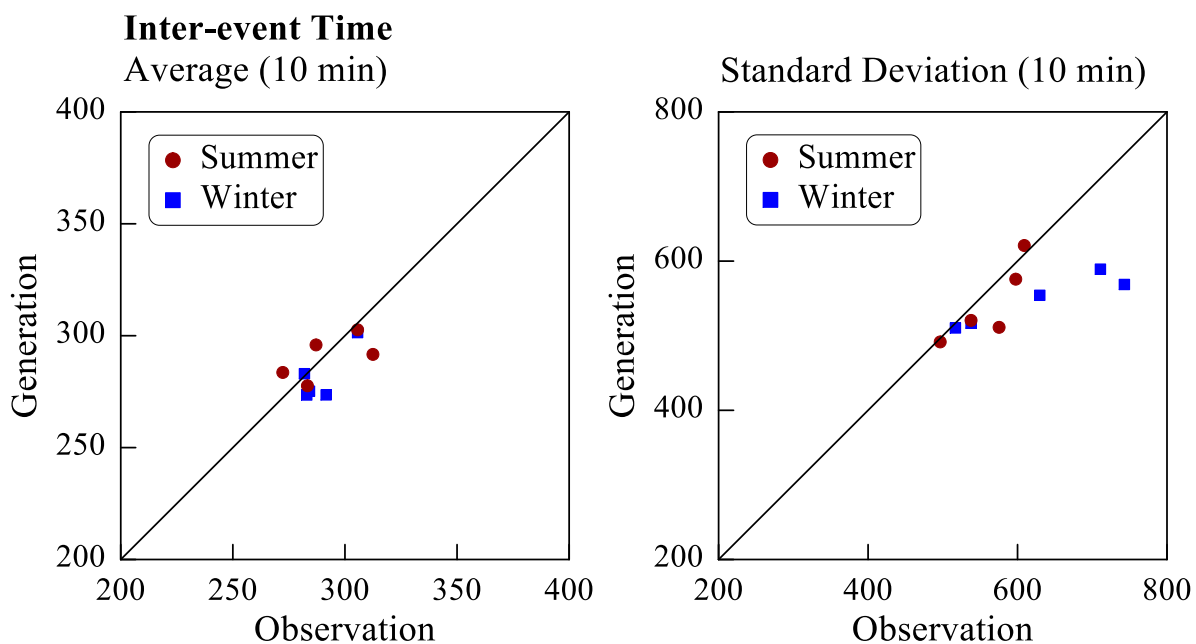


Figure 13. Comparison of the average and standard deviation values obtained for the observed and generated inter-event times.

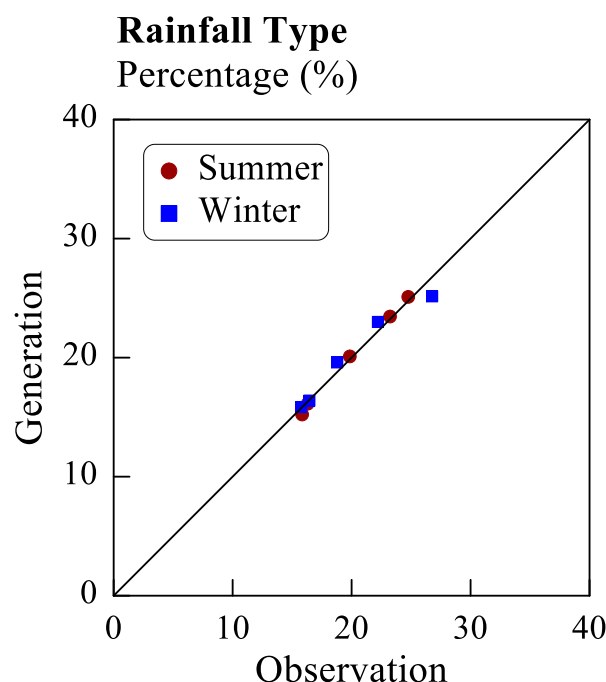


Figure 14. Comparison of the observed and generated numbers of rainfall events for different rainfall types.

6. Conclusions

This paper proposes a stochastic rainfall generator for producing a continuous rainfall time series with high temporal resolution. Observed 10 min rainfall time series from 2012 to 2018 for the Yilan River Basin in Taiwan were collected, and the rainfall events identified in the collected data were divided into summer and winter rainfall events (4317 and 3246 events, respectively). Although the stochastic rainfall-generation process adopted in the proposed generator is based on conventional Monte Carlo simulation, the use of modified Huff curves and a copula enables the generated rainfall series to exhibit appropriate rainfall types and precise correlation between rainfall quantity and rainfall duration.

The modified Huff method not only overcomes the limitation related to classifying rainfall events with multiple peak intensities but also includes a new rainfall type for labeling rainfall events with uniform temporal distribution. The Schutz index was used in this study to distinguish this new rainfall type, which is ignored in the traditional Huff method. The modified Huff method reduced the number of omitted rainfall events in the study area from 40% (with the conventional Huff method) to 5%. Moreover, a copula was used to model the correlation between each pair among three rainfall parameters in the generation process. The results indicated that the rainfall quantity and duration were correlated. Three copulas from the Archimedean family were used in this study, and the Frank copula was found to be the optimal copula for modeling the correlation between rainfall quantity and rainfall duration.

The proposed stochastic rainfall generator was used to generate a continuous rainfall time series with 10,000 sets of alternating rainfall events and inter-event times. The generated rainfall time series was assessed by comparing its statistical indices with those of the observed rainfall data. The results of this comparison indicated that the mean values obtained for the generated and observed rainfall quantity, duration, and inter-event time were similar. The standard deviations of the generated rainfall quantity and duration were close to those of the observed rainfall quantity and duration, respectively. Only the standard deviation of the rainfall inter-event time in winter was marginally underestimated. By using the Frank copula, the correlation between rainfall quantity and rainfall duration

can be suitably preserved in the rainfall time series generated using the proposed stochastic rainfall generator. Moreover, the differences between the statistical properties of Type 5 rainfall events and other types of rainfall events support the rationality and necessity of using the modified Huff rainfall curves adopted in this study. In summary, the results of this study indicate that the developed stochastic rainfall generator can accurately reproduce continuous rainfall time series with a temporal resolution of 10 min.

Nonetheless, some issues are discussed in the following as potential improvements for future works. This study used all collected rainfall observations to examine the performance of the rainfall generator. Future work may conduct the cross-validation scheme to check the generation performance with respect to a certain period or a particular site. This study adopted the bivariate copula due to the correlation relationship among the rainfall variables in the study area. The trivariate copula can be tested to model the correlation among multiple variables. This study proposed an additional rainfall type on the basis of Huff rainfall curves, and analysis results demonstrated the success of the modified Huff method. However, the temporal distribution of rainfall events are not certainly restricted to the five types of modified Huff model in this study. Alternative rainfall type methods can be adopted in generating the rainfall time series. The proposed rainfall generator focused on reproducing the rainfall time series with correct statistical characteristics. The spatial rainfall feature was not considered herein. Future works can focus on developing a rainfall generator accounting for the spatial and temporal characteristics simultaneously.

Author Contributions: Conceptualization, S.-T.C.; formal analysis, D.T.N. and S.-T.C.; methodology, D.T.N. and S.-T.C.; visualization, S.-T.C.; writing—original draft, D.T.N. and S.-T.C.; writing—review and editing, S.-T.C. All authors have read and agreed to the published version of the manuscript.

Funding: This research received no external funding.

Institutional Review Board Statement: Not applicable.

Informed Consent Statement: Not applicable.

Conflicts of Interest: The authors declare no conflict of interest.

References

1. Breinl, K. Driving a lumped hydrological model with precipitation output from weather generators of different complexity. *Hydrol. Sci. J.* **2016**, *61*, 1395–1414. [[CrossRef](#)]
2. Chlumecký, M.; Buchtele, J.; Richta, K. Application of random number generators in genetic algorithms to improve rainfall-runoff modelling. *J. Hydrol.* **2017**, *553*, 350–355. [[CrossRef](#)]
3. Candela, A.; Brigandì, G.; Aronica, G.T. Estimation of synthetic flood design hydrographs using a distributed rainfall-runoff model coupled with a copula-based single storm rainfall generator. *Nat. Hazards Earth Syst. Sci.* **2014**, *14*, 1819–1833. [[CrossRef](#)]
4. Winter, B.; Schneeberger, K.; Dung, N.V.; Huttenlau, M.; Achleitner, S.; Stötter, J.; Merz, B.; Vorogushyn, S. A continuous modelling approach for design flood estimation on sub-daily time scale. *Hydrol. Sci. J.* **2019**, *64*, 539–554. [[CrossRef](#)]
5. Chimene, C.A.; Campos, J.N.B. The design flood under two approaches: Synthetic storm hyetograph and observed storm hyetograph. *J. Appl. Water Eng. Res.* **2020**, *8*, 171–182. [[CrossRef](#)]
6. Chen, S.T.; Yu, P.S.; Tang, Y.H. Statistical downscaling of daily precipitation using support vector machines and multivariate analysis. *J. Hydrol.* **2010**, *385*, 13–22. [[CrossRef](#)]
7. Yang, T.C.; Yu, P.S.; Wei, C.M.; Chen, S.T. Projection of climate change for daily precipitation: A case study in Shih-Men Reservoir catchment in Taiwan. *Hydrol. Processes* **2011**, *25*, 1342–1354. [[CrossRef](#)]
8. Khazaei, M.R.; Zahabiyoun, B.; Saghafian, B. Assessment of climate change impact on floods using weather generator and continuous rainfall-runoff model. *Int. J. Climatol.* **2012**, *32*, 1997–2006. [[CrossRef](#)]
9. Tukimat, N.N.A.; Syukri, N.A.; Malek, M.A. Projection the long-term ungauged rainfall using integrated Statistical Downscaling Model and Geographic Information System (SDSM-GIS) model. *Heliyon* **2019**, *5*, e02456. [[CrossRef](#)]
10. Grimaldi, S.; Nardi, F.; Piscopia, R.; Petroselli, A.; Apollonio, C. Continuous hydrologic modelling for design simulation in small and ungauged basins: A step forward and some tests for its practical use. *J. Hydrol.* **2021**, *595*, 125664. [[CrossRef](#)]
11. Katz, R.W. Precipitation as a chain-dependent process. *J. Appl. Meteorol.* **1977**, *16*, 671–676. [[CrossRef](#)]
12. Richardson, C.W. Stochastic simulation of daily precipitation, temperature, and solar radiation. *Water Resour. Res.* **1981**, *17*, 182–190. [[CrossRef](#)]
13. Westra, S.; Mehrotra, R.; Sharma, A.; Srikanthan, R. Continuous rainfall simulation: 1. A regionalized subdaily disaggregation approach. *Water Resour. Res.* **2012**, *48*, W01535. [[CrossRef](#)]

14. De Luca, D.L.; Petroselli, A. STORAGE (STOchastic RAInfall GEnerator): A user-friendly software for generating long and high-resolution rainfall time series. *Hydrology* **2021**, *8*, 76. [CrossRef]
15. Keifer, C.J.; Chu, H.H. Synthetic storm pattern for drainage design. *J. Hydraul. Div.* **1957**, *83*, 1–25. [CrossRef]
16. Huff, F.A. Time distribution of rainfall in heavy storms. *Water Resour. Res.* **1967**, *3*, 1007–1019. [CrossRef]
17. Yen, B.C.; Chow, V.T. Design hyetographs for small drainage structures. *J. Hydraul. Div.* **1980**, *106*, 1055–1076. [CrossRef]
18. Rodriguez-Iturbe, I.; Cox, D.R.; Isham, V. Some models for rainfall based on stochastic point processes. *Proc. R. Soc. London. A. Math. Phys. Sci.* **1987**, *410*, 269–288.
19. Rodriguez-Iturbe, I.; De Power, B.F.; Valdes, J.B. Rectangular pulses point process models for rainfall: Analysis of empirical data. *J. Geophys. Res. Atmos.* **1987**, *92*, 9645–9656. [CrossRef]
20. Entekhabi, D.; Rodriguez-Iturbe, I.; Eagleson, P.S. Probabilistic representation of the temporal rainfall process by a modified Neyman-Scott rectangular pulses model: Parameter estimation and validation. *Water Resour. Res.* **1989**, *25*, 295–302. [CrossRef]
21. Cowpertwait, P.S. Further developments of the Neyman-Scott clustered point process for modeling rainfall. *Water Resour. Res.* **1991**, *27*, 1431–1438. [CrossRef]
22. Sørup, H.J.D.; Christensen, O.B.; Arnbjerg-Nielsen, K.; Mikkelsen, P.S. Downscaling future precipitation extremes to urban hydrology scales using a spatio-temporal Neyman-Scott weather generator. *Hydrol. Earth Syst. Sci.* **2016**, *20*, 1387–1403. [CrossRef]
23. Cowpertwait, P.S.P.; Kilsby, C.G.; O’Connell, P.E. A space-time Neyman-Scott model of rainfall: Empirical analysis of extremes. *Water Resour. Res.* **2022**, *38*, 1131. [CrossRef]
24. Lee, J.; Kim, U.; Kim, S.; Kim, J. Development and application of a rainfall temporal disaggregation method to project design rainfalls. *Water* **2022**, *14*, 1401. [CrossRef]
25. De Luca, D.L.; Apollonio, C.; Petroselli, A. The benefit of continuous hydrological modelling for drought hazard assessment in small and coastal ungauged basins: A case study in Southern Italy. *Climate* **2022**, *10*, 34. [CrossRef]
26. Islam, S.; Entekhabi, D.; Bras, R.L.; Rodriguez-Iturbe, I. Parameter estimation and sensitivity analysis for the modified Bartlett-Lewis rectangular pulses model of rainfall. *J. Geophys. Res. Atmos.* **1990**, *95*, 2093–2100. [CrossRef]
27. Onof, C.; Wheater, H.S. Modelling of British rainfall using a random parameter Bartlett-Lewis rectangular pulse model. *J. Hydrol.* **1993**, *149*, 67–95. [CrossRef]
28. Khaliq, M.N.; Cunnane, C. Modelling point rainfall occurrences with the modified Bartlett-Lewis rectangular pulses model. *J. Hydrol.* **1996**, *180*, 109–138. [CrossRef]
29. Onof, C.; Wang, L.P. Modelling rainfall with a Bartlett-Lewis process: New developments. *Hydrol. Earth Syst. Sci.* **2020**, *24*, 2791–2815. [CrossRef]
30. Islam, M.A.; Yu, B.; Cartwright, N. Coupling of satellite-derived precipitation products with Bartlett-Lewis model to estimate intensity-frequency-duration curves for remote areas. *J. Hydrol.* **2022**, *609*, 127743. [CrossRef]
31. Rafatnejad, A.; Tavakolifar, H.; Nazif, S. Evaluation of the climate change impact on the extreme rainfall amounts using modified method of fragments for sub-daily rainfall disaggregation. *Int. J. Climatol.* **2022**, *42*, 908–927. [CrossRef]
32. Huff, F.A.; Vogel, J.L. Hydrometeorology of Heavy Rainstorms in Chicago and Northeastern Illinois, Phase I—Historical Studies, Illinois State Water Survey. 1976. Available online: <http://hdl.handle.net/2142/77792> (accessed on 15 May 2022).
33. Huff, F.A. Time Distributions of Heavy Rainstorms in Illinois. Circular No. 173; Department of Energy and Natural Resources, State of Illinois. 1990. Available online: <https://www.ideals.illinois.edu/bitstream/handle/2142/94492/ISWSC-173.pdf?sequence=1> (accessed on 15 May 2022).
34. Yu, P.S.; Chen, S.T.; Chen, C.J.; Yang, T.C. The potential of fuzzy multi-objective model for rainfall forecasting from typhoons. *Nat. Hazards* **2005**, *34*, 131–150. [CrossRef]
35. Azli, M.; Rao, A.R. Development of Huff curves for peninsular Malaysia. *J. Hydrol.* **2010**, *388*, 77–84. [CrossRef]
36. Golian, S.; Saghafian, B.; Maknoon, R. Derivation of probabilistic thresholds of spatially distributed rainfall for flood forecasting. *Water Resour. Manag.* **2010**, *24*, 3547–3559. [CrossRef]
37. Chen, S.T. Multiclass support vector classification to estimate typhoon rainfall distribution. *Disaster Adv.* **2013**, *6*, 110–121.
38. Dolšak, D.; Bezak, N.; Šraj, M. Temporal characteristics of rainfall events under three climate types in Slovenia. *J. Hydrol.* **2016**, *541*, 1395–1405. [CrossRef]
39. Wartalska, K.; Kaźmierczak, B.; Nowakowska, M.; Kotowski, A. Analysis of hyetographs for drainage system modeling. *Water* **2020**, *12*, 149. [CrossRef]
40. Dunkerley, D. Regional rainfall regimes affect the sensitivity of the Huff quartile classification to the method of event delineation. *Water* **2022**, *14*, 1047. [CrossRef]
41. Sklar, M. Fonctions de repartition an dimensions et leurs marges. *Publ. Inst. Statist. Univ. Paris* **1959**, *8*, 229–231.
42. De Michele, C.; Salvadori, G. A generalized Pareto intensity-duration model of storm rainfall exploiting 2-copulas. *J. Geophys. Res. Atmos.* **2003**, *108*, 4067. [CrossRef]
43. Favre, A.C.; El Adlouni, S.; Perreault, L.; Thiémondge, N.; Bobée, B. Multivariate hydrological frequency analysis using copulas. *Water Resour. Res.* **2004**, *40*, W01101. [CrossRef]
44. Kao, S.C.; Chang, N.B. Copula-based flood frequency analysis at ungauged basin confluences: Nashville, Tennessee. *J. Hydrol. Eng.* **2012**, *17*, 790–799. [CrossRef]

45. Dodangeh, E.; Singh, V.P.; Pham, B.T.; Yin, J.; Yang, G.; Mosavi, A. Flood frequency analysis of interconnected Rivers by copulas. *Water Resour. Manag.* **2020**, *34*, 3533–3549. [[CrossRef](#)]
46. Pathak, A.A.; Dodamani, B.M. Connection between meteorological and groundwater drought with copula-based bivariate frequency analysis. *J. Hydrol. Eng.* **2021**, *26*, 05021015. [[CrossRef](#)]
47. Razmkhah, H.; Fararouie, A.; Ravari, A.R. Multivariate flood frequency analysis using bivariate copula functions. *Water Resour. Manag.* **2022**, *36*, 729–743. [[CrossRef](#)]
48. Jang, J.H.; Chang, T.H. Flood risk estimation under the compound influence of rainfall and tide. *J. Hydrol.* **2022**, *606*, 127446. [[CrossRef](#)]
49. Genest, C.; Rivest, L.P. On the multivariate probability integral transformation. *Stat. Probab. Lett.* **2001**, *53*, 391–399. [[CrossRef](#)]
50. Kao, S.C.; Govindaraju, R.S. Trivariate statistical analysis of extreme rainfall events via the Plackett family of copulas. *Water Resour. Res.* **2008**, *44*, W02415. [[CrossRef](#)]
51. Kao, S.C.; Govindaraju, R.S. A copula-based joint deficit index for droughts. *J. Hydrol.* **2010**, *380*, 121–134. [[CrossRef](#)]
52. Amirataee, B.; Montaseri, M.; Rezaie, H. An advanced data collection procedure in bivariate drought frequency analysis. *Hydrol. Processes* **2020**, *34*, 4067–4082. [[CrossRef](#)]
53. Salvadori, G.; De Michele, C. Frequency analysis via copulas: Theoretical aspects and applications to hydrological events. *Water Resour. Res.* **2004**, *40*, W12511. [[CrossRef](#)]
54. Salvadori, G.; De Michele, C. On the use of copulas in hydrology: Theory and practice. *J. Hydrol. Eng.* **2007**, *12*, 369–380. [[CrossRef](#)]
55. Genest, C.; Favre, A.C. Everything you always wanted to know about copula modeling but were afraid to ask. *J. Hydrol. Eng.* **2007**, *12*, 347–368. [[CrossRef](#)]
56. Gao, C.; Xu, Y.P.; Zhu, Q.; Bai, Z.; Liu, L. Stochastic generation of daily rainfall events: A single-site rainfall model with copula-based joint simulation of rainfall characteristics and classification and simulation of rainfall patterns. *J. Hydrol.* **2018**, *564*, 41–58. [[CrossRef](#)]
57. Vandenberghe, S.; Verhoest, N.E.C.; De Baets, B. Properties and performance of a copula-based design storm generator. In Proceedings of the International workshop: Advances in Statistical Hydrology, Taormina, Italy, 23–25 May 2010.
58. Schutz, R.R. On the measurement of income inequality. *Am. Econ. Rev.* **1951**, *41*, 107–122.
59. Lorenz, M.O. Methods of measuring the concentration of wealth. *Publ. Am. Stat. Assoc.* **1905**, *9*, 209–219. [[CrossRef](#)]
60. Cameron, D.; Beven, K.; Naden, P. Flood frequency estimation by continuous simulation under climate change (with uncertainty). *Hydrol. Earth Syst. Sci.* **2020**, *4*, 393–405. [[CrossRef](#)]
61. Sharafati, A.; Zahabiyoun, B. Stochastic generation of storm pattern. *Life Sci. J.* **2013**, *10*, 1575–1583.
62. Bonta, J.V.; Rao, A.R. Factors affecting the identification of independent storm events. *J. Hydrol.* **1988**, *98*, 275–293. [[CrossRef](#)]
63. Vernieuwe, H.; Vandenberghe, S.; De Baets, B.; Verhoest, N. A continuous rainfall model based on vine copulas. *Hydrol. Earth Syst. Sci.* **2015**, *19*, 2685–2699. [[CrossRef](#)]
64. Bonta, J.V.; Shahalam, A. Cumulative storm rainfall distributions: Comparison of Huff curves. *J. Hydrol.* **2003**, *42*, 65–74.